Synthesis of Potassium-Modified Graphene and Its Application in Nitrite-Selective Sensing

Xiao-Rong Li, Fen-Ying Kong, Jing Liu, Tong-Ming Liang, Jing-Juan Xu, and Hong-Yuan Chen*

Chemical modification with foreign atoms is a leading strategy to intrinsically modify the properties of host materials. Among them, potassium (K) modification plays a critical role in adjusting the electronic properties of carbon materials. Graphene, a true 2D carbon material, has shown fascinating applications in electrochemical sensing and biosensing. In this work, a facile and mild strategy to K-modifying in graphene at room-temperature is reported for the first time. X-ray photoelectron spectroscopy (XPS), atomic force microscopy (AFM), transmission electron microscopy (TEM), Raman spectra, and cyclic voltammetry are used to characterize this K-modified graphene. The K-modified graphene is capable of acting as an electron transfer medium and more efficiently promotes charge transfer than unmodified graphene. A highly sensitive and stable amperometric sensor based on its excellent electrocatalytic activity toward the oxidation of NO_2^- is proposed. The sensor shows a linear range from 0.5 μM to 7.8 mM with a detection limit of 0.2 μM at a signal-to-noise ratio of 3. The modified electrode has excellent analytical performance and can be successfully applied in the determination of NO_2^- released from liver cancer and leukemia cells and shows good application potential in biological systems.

1. Introduction

Since the discovery of graphene by Geim et al. in 2004,[1] it has been touted as a "rising star" material because of its remarkable properties, including electronic, optical, and thermal properties; chemical and mechanical stability; and large surface area.[1–11] These physical and chemical properties hold great promise for its potential applications in many technological fields such as nanoelectronics,[12,13] nanophotonics,[14] nanocomposites,[15,16] electric devices,[17] and sensors.[18] Recently, tailoring and developing the electronic characteristics of graphene to achieve unique properties has attracted great attention.[19–21] Electronic properties of graphene have been altered by chemical functionalization and electrochemical modification.[22,23] Many hybrids, such as graphene/polymer nanocomposites,[24] graphene/metal nanoparticle sheets,[25–28] and graphene/metal oxide deposits,[29] have been reported. However, most of these methods have been aimed at obtaining graphene hybrids with synergy or multiple functionalities. Little attention has been paid to intrinsic modification of graphene with the purpose of enhancing the graphene performance in electrochemical sensing and biosensing systems.

Chemical modification with foreign atoms is an effective method to intrinsically modify the properties of host materials, including the electronic, magnetic, chemical, and mechanical properties. For carbon materials, chemical modification is a leading potential strategy to enrich free charge-carrier densities and enhance the electrical or thermal conductivities.[19] Recently, many studies have demonstrated the achievements of chemical modification of graphene.[30,31] For example, by using an oxygen etching process, graphene is simultaneously etched and modified by oxidation.[32] By using nitrogen plasma treatment method, N-modified graphene is obtained by exposing graphene to nitrogen plasma.[19,33] Theoretical investigation of metal-modified graphene has predicted the possibility of a Fermi level shift and a crossover from p-type to n-type.[34] Among the numerous potential modifiers, the alkali metal modification, such as potassium (K), is considered to be an excellent element for the chemical modification of carbon materials and expected to modify the electronic properties of graphene. So far, only two studies aimed at producing K-modified graphene with vaporized K[35] and chemical vapor deposition,[36] respectively, in a high vacuum system at high temperature, which makes graphene restack more easily. Additionally, with the two methods it is difficult to control the modifying concentration and they need high-energy consumption. As a result, an alternative modification strategy should be developed. In previous work, the room-temperature chemical K modification has been successfully employed to modify the electrical or chemical properties of carbon nanotubes (CNTs). For instance, the room-temperature chemical K modification of CNTs increases

X.-R. Li, F.-Y. Kong, J. Liu, T.-M. Liang, Prof. J.-J. Xu, H.-Y. Chen
State Key Laboratory of Analytical Chemistry for Life Science
School of Chemistry and Chemical Engineering
Nanjing University
Nanjing 210093, China
E-mail: xujj@nju.edu.cn

DOI: 10.1002/adfm.201103025

the metallic behavior, affects the lattice alignment, and regulates the electrical, mechanical, and chemical properties.[37] Moreover, it has been demonstrated that K modification enhanced the biocompatibility and sensitivity of CNTs in biosensing applications.[38] Consequently, the room-temperature chemical K-modifying has great potential to be used for graphene modification.

Nitrite (NO_2^-) has been widely exploited in our daily life as food addditives, excessively disposed into the ecosystem, and recognized as an alarming pollutant to the environment and human health. In natural ecosystems NO_2^- is of interest because of its toxicity for microorganisms and higher organisms.[39] The World Health Organization has reported that the fatal dose of nitrite ingestion is between 8.7 μM and 28.3 μM.[40] NO_2^- is a major oxidation product derived from NO that is produced in a wide variety of cell types by NO synthases.[41] Moreover, NO_2^- accumulated in the human body may cause methemoglobinemia and, furthermore, may become source of carcinogenic N-nitrosamines.[42,43] As a consequence, accurate, rapid, and economic determination of NO_2^- has attracted much attention. Many methods have been developed to detect nitrite, such as electrochemical biosensors,[44,45] spectrophotometry,[46,47] gas chromatography-mass spectrometry,[48] ion chromatography,[49] spectrofluorimetry,[50,51] chemiluminescence,[52] flow injection analysis,[53] and capillary electrophoresis.[54] Among these methods, electrochemical techniques are proven to be powerful tools due to their rapid response and simple operation. In the recent years, NO_2^- biosensors have been widely reported using many heme proteins, for example hemoglobin, nitrite reductase, and myoglobin.[55–57] These biosensors are mainly ascribed to the electroreductive reactions of NO_2^-. The reduction of NO_2^- yielded several products depending on the electrode conditions and the nature of the catalyst employed, and its anodic oxidation is a straightforward reaction, with NO_3^- as the final product. Hence, anodic NO_2^- determination has attracted great attention because it offers several advantages, in particular with no interference. In contrast, the major limitations of cathodic determination of NO_2^- is due to interference from NO and O_2. It is therefore important to exploit a novel electrode material for the oxidation of NO_2^- as well as to develop a highly selective sensor with micromolar or even nanomolar sensitivity to provide quantitative information on NO_2^- concentrations for tracking the role that NO_2^- plays in physiological and pathological processes.

In this work, we report a facile and mild strategy to synthesize K-modified graphene using a room-temperature chemical method that is a simple and controllable approach for material surface modification and can be used for the introduction of foreign atoms, groups, or structures onto bulk scaffold surfaces. The resulting K-modified graphene can act as an electron transfer medium and more efficiently promotes charge transfer than unmodified graphene. NO_2^- shows excellent electrochemical response at the K-modified graphene glassy carbon electrode (GCE), thus leading to a highly sensitive NO_2^- amperometric sensor. The developed sensor is successfully applied in the determination of NO_2^- released from liver cancer and leukemia cells. Therefore, the room-temperate chemical K-modified graphene provides a convenient way with great promise for electrochemical sensors and biosensors design and extends the application of graphene in bioanalysis.

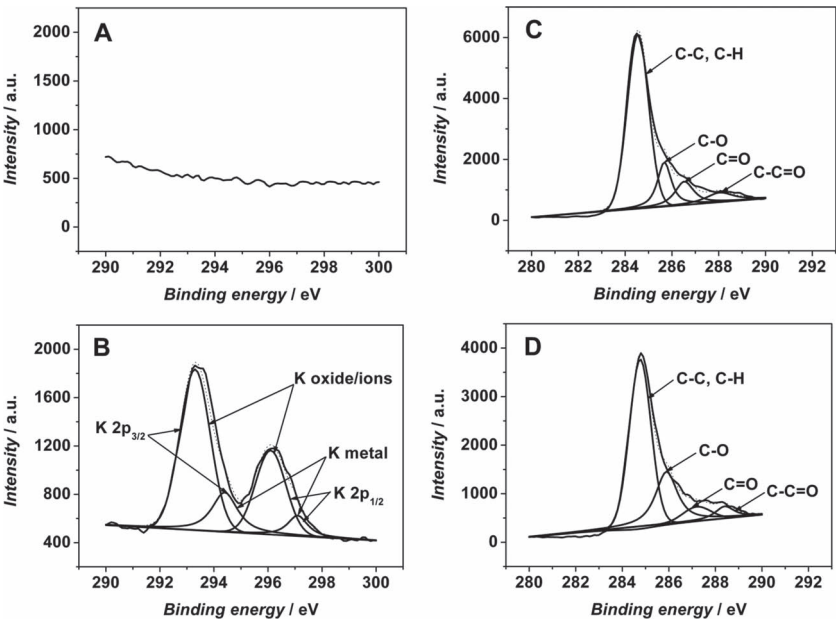

Figure 1. XPS K 2p spectra of A) graphene and B) K-modified graphene. C 1s spectra of C) graphene and D) K-modified graphene.

2. Results and Discussion

2.1. Characterization of K-Modified Graphene

X-ray photoelectron spectroscopy (XPS) is a powerful tool to identify the states of the elements in bulk material. According to the analysis of binding energy (BE) values, we can confirm the nature of the binding between carbon and potassium. As shown in **Figure 1**A, no K peaks are observed for graphene. However, K peaks in the spectra of K-modified graphene are observed at BE = 293.2 eV (K $2p_{3/2}$) and 296.0 eV (K $2p_{1/2}$) (Figure 1B). The two peaks correspond to a spin-orbit split doublet, which can be attributed to the K oxides and cations, respectively.[37,58,59] Thus, only K species is observed in the metal-modifying process. The highly reactive K atoms can readily react with the surface migrated oxygen from the bulk of graphene to form an oxidized interfacial layer. K cations, resulting from charge transfer interaction between the K atoms and graphene backbone, may also have contributed in part to this peak component. At higher coverage of K, the K 2p core-level spectrum also reveals the contribution of the metallic K, with the BE for its K $2p_{3/2}$ and K $2p_{1/2}$ peaks component lying at about 294.4 and 297.1 eV.[58,59] The result is in agreement with the intercalation by substitution, which is based on an ion transfer rather than on an electron transfer, as is shown to

happen in the intercalation by reduction.[37,60] The K-modifying concentration varies from 2.39 to 8.72 at% according to the elemental sensitivity factors method,[61] and it changes sensitively by controlling the initial amount of K in the synthesis procedure, as shown in **Figure 2**, indicating a controllable modification of K in the graphene. The K-modifying concentration increased significantly as the initial amount of K increased from 10 to 40 mg, then slowly changed from 40 to 100 mg and reached the relatively stable value. Such K species would decorate the graphene planar sheet and might introduce a change in the Fermi level and charge transfer, producing the modifying effects and opening the bandgap of the graphene. As a consequence, K modification might play an important role in regulating the electronic properties and enhancing the electrocatalytic activity of graphene in electrochemical systems. Finally, the initial amount of 40 mg K was chosen as a standard synthesis for K-modified graphene and the resulting K-modified graphene was used for further investigation with the K-modifying concentration of 6.97 at% in the graphene.

XPS of C 1s ranging from 280 to 290 eV are shown in Figure 1C,D. The C 1s strong peak at 284.6 eV, which is consistent with sp^2 graphite carbon, did not significantly change, but the at% of the C 1s of the K-modified graphene was reduced by 13.67 at% compared with that of the unmodified graphene. The C 1s spectra is composed of a major peak at 284.6 eV, which is associated with the C–C and C–H bonding, and three minor peaks at ≈285.9 eV, 287.0 eV, and 288.8 eV, which correspond to the C–O, C=O, and C–C=O, respectively.[19] The oxidized carbon species are induced by the K oxides and the reactive nature of graphene in the air environment, which indicates that the K modification enhanced the charge transfer interaction between the carbon atoms and the oxygen atoms. Meanwhile, K modification might change the nature structure of functional oxygen in graphene. XPS spectra of O 1s before and after K modification are shown in **Figure 3**A,B (C–O at 533.9 eV, C=O at 532.5 eV, and O–C=O at 531.6 eV).[19,62] After K modification, the oxygen content was 22.82 at%, which is higher than the unmodified graphene (16.12 at%).

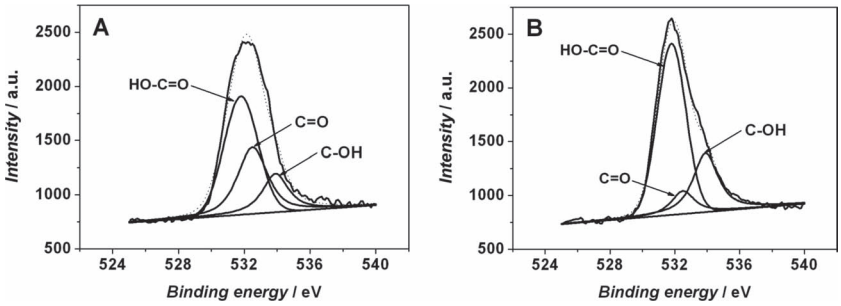

Figure 3. XPS O 1s spectra of A) graphene and B) K-modified graphene.

The atomic force microscopy (AFM) images were used to characterize the chemically synthesized graphene and K-modified graphene sheets. As shown in **Figure 4**A, the thickness of graphene sheet was measured to be about 0.8 nm. Considering that the thickness of a clean graphene sheet is 0.7 nm,[63] the thickness was close to that of a single layer graphene sheet. However, after K-modifying, the thickness of the K-modified graphene sheet was found to be in the range of 0.8–1.1 nm (Figure 4B) due to the introduction of K in the graphene; it could be concluded that K species, including K cations (296.0 eV), K oxides (293.2 eV), and K metal (294.4 and 297.1 eV), were assembled on a monolayer of graphene sheet. Meanwhile, such K species decorated the graphene planar sheet, resulting in a rough and slightly undulating surface. Furthermore, the low-magnification transmission electron microscopy (TEM) image revealed few-layer flexible wrinkled sheets of the graphene situated on the top of the copper grid (**Figure 5**A), illustrating the flake-like shape of graphene.[64–66] Moreover, the graphene planar sheets can be observed clearly in K-modified graphene (Figure 5B), indicating that the features of high surface to volume ratio and 2D structure of graphene morphology are well maintained. High-resolution transmission electron microscopy (HRTEM) images also reveal the monolayer planar structure in the graphene (Figure 5C) and K-modified graphene (Figure 5D). To determine the crystallinity of the graphene sheets, the corresponding selected-area electron diffraction (SAED) pattern was also examined. The inset of Figure 5C shows the SAED pattern where only one set of symmetric hexagonal diffraction spots are detected, which are the typical hexagonal lattice of carbon in graphene. It indicates that the graphene sheet is a single crystalline domain within the selected area.[67,68] However, unlike the graphene sheets of symmetric hexagonal diffraction patterns, the SAED of the K-modified graphene (inset of Figure 5D) shows a weak halo with blurred hexagonal diffraction spots. The observed difference indicates that the crystalline graphene sheets became partially misorientated in the K-modified graphene due to structure distortions caused by the intercalation of K species into the graphite plane. Meanwhile, the weak diffraction pattern suggests that the metal species are randomly dispersed in the graphene without azimuthal correlation but with a fixed metal–carbon distance.[69] Furthermore, a DC resistance measurement was carried out to investigate the

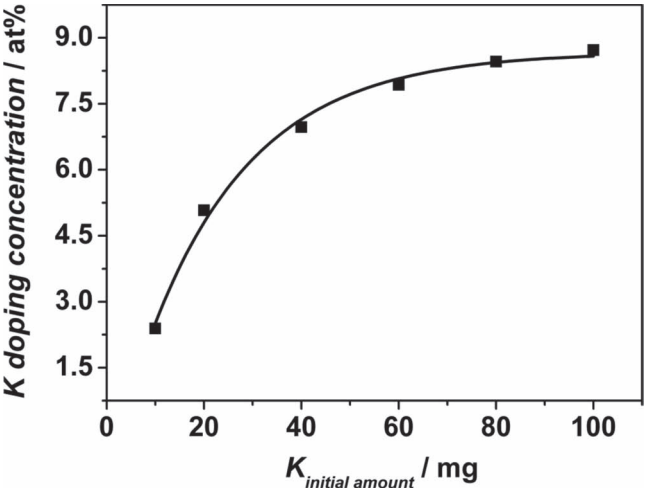

Figure 2. Dependence of the at% of K modifying concentration estimated from XPS analysis of the initial amount of K in the synthesis process.

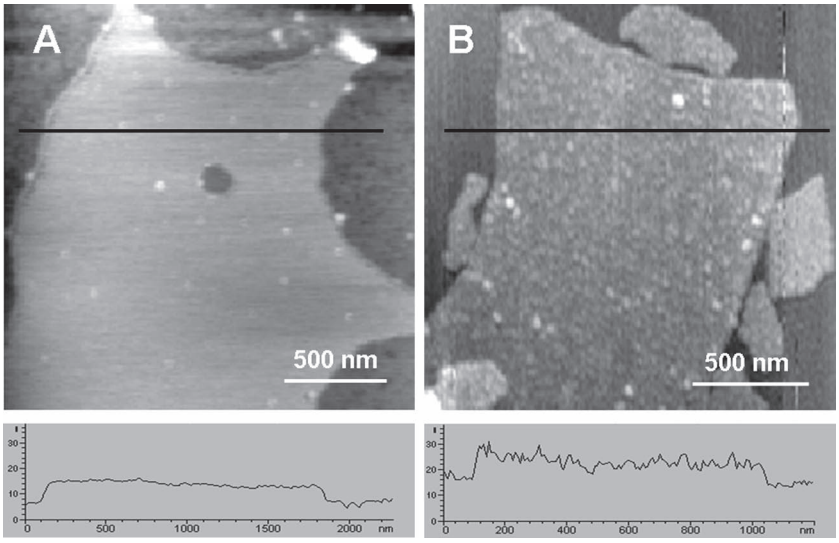

Figure 4. AFM images of A) graphene and B) K-modified graphene. The correpsonding height analyses along the lines marked in the AFM images.

conductivity of graphene and K-modified graphene. As shown in **Figure 6**, for both graphene and K-modified graphene, the conductivity increased significantly as the temperature increased from 10 to 50 K, then slowly increased from 50 to 300 K. Meanwhile, the K-modified graphene exhibits much higher electrical conductivity than that of the unmodified one in the whole temperature range.

The Raman spectrum of graphene showed a disorder-induced D band at 1346 cm^{-1} arising from sp^3-hybridized carbon and a tangential stretch G band at 1576 cm^{-1} representing the E_{2g} zone center mode of the crystalline graphite (curve a, **Figure 7**A), which is indicative of a significant number of edge-plane-like defective sites on the surface of graphene.[70,71] The 2D band of graphene was at 2687 cm^{-1}, which is the most prominent feature in the Raman spectrum of graphene; its shape is highly sensitive and can be used to identify single-layer and few-layer graphene.[72] In this spectrum, the 2D peak is a symmetric and sharp peak, shifting toward monolayer graphene, whereas bilayer and few-layer graphene have broader and blue-shifted 2D bands compared to the monolayer graphene.[73,74] In addition, K-modified graphene had a 2D band at a lower frequency (2683 cm^{-1}) with the same symmetric and sharp shape (curve b, Figure 7A). This suggests that the number of layers in the K-modified graphene was close to monolayer. Additionally, compared to the graphene, the relatively increased intensity of the disorder mode suggested that the incorporation of K brought about a change in the degree of ordering in the hexagonal framework of graphene.[37,75,76] The Raman spectrum of the K-modified graphene showed a disorder-induced D band at 1350 cm^{-1} and a tangential stretch G band at 1579 cm^{-1} (curve b, Figure 7A), with an intensity ratio I_D/I_G = 0.97. This value was much higher than the 0.70 observed for graphene. As a consequence, we found that K modification was very effective at introducing defects into the structure of the graphene.

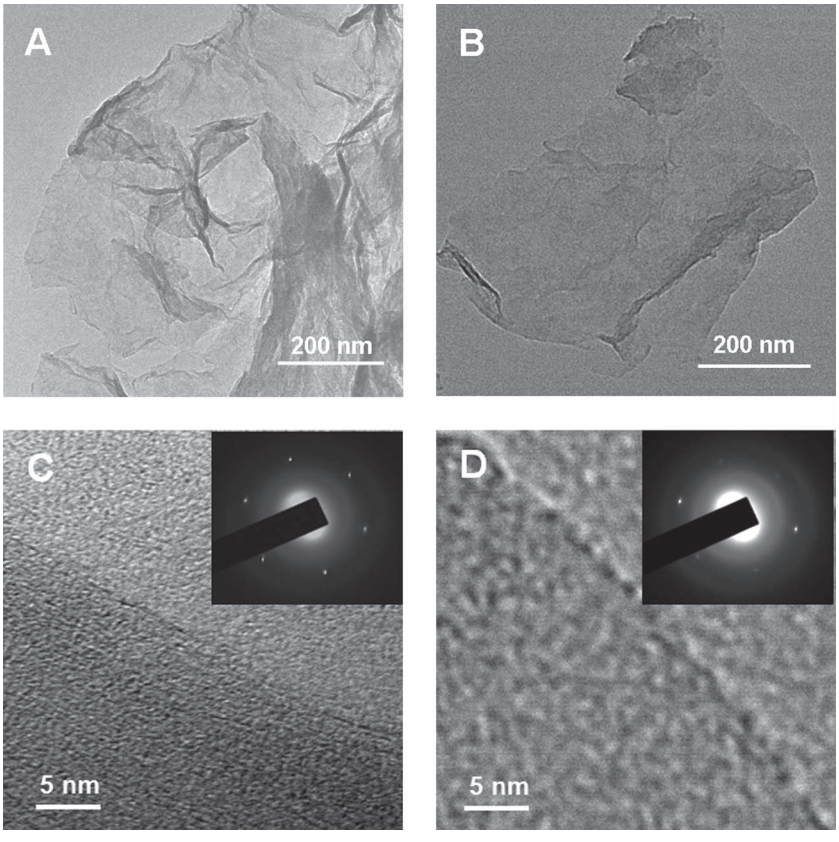

Figure 5. Low-resolution TEM images of A) graphene and B) K-modified graphene. HRTEM images of C) graphene and D) K-modified graphene with the corresponding SAED patterns (insets).

Furthermore, to investigate the effect of the K-modified graphene on the electron transfer kinetics of the redox probe at the electrode surface, the cyclic voltammograms of the K-modified graphene/GCE in 0.1 M KCl solution containing 5 mM $K_3[Fe(CN)_6]/K_4[Fe(CN)_6]$ is shown in curve c (Figure 7B). The peak currents increased compared with those of the graphene/GCE (curve b, Figure 7B) and bare GCE (curve a, Figure 7B). The potential differences of the peak-to-peak (D_{EP}) at the K-modified graphene, graphene, and bare GCE were 96, 106, and 117 mV, respectively. Both the small differences between these D_{EP} and the changes in peak currents showed that the K-modified graphene effectively accelerates the electron transfer between $Fe(CN)_6^{3-/4-}$ and the electrode.

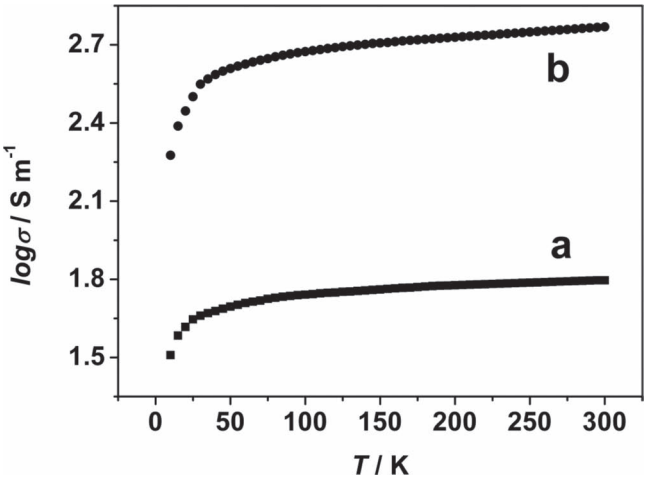

Figure 6. Electrical conducting data of graphene (a) and K-modified graphene (b).

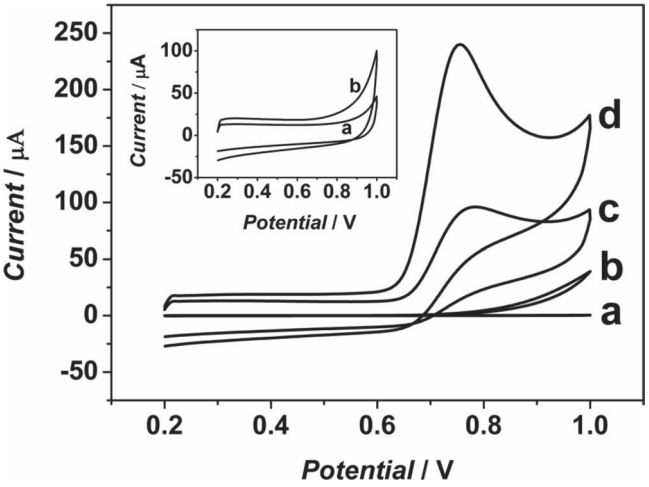

Figure 8. Cyclic voltammograms of bare/GCE (a,b), graphene/GCE (c), and K-modified graphene/GCE (d) in the absence (a) and presence (b,c,d) of 5 mM NO_2^- in 0.1 M pH 7.4 PBS. Inset: Cyclic voltammograms of graphene/GCE (a) and K-modified graphene/GCE (b) in 0.1 M pH 7.4 PBS. Scan rate: 50 mV s^{-1}.

2.2. Electrocatalysis of K-Modified Graphene

To explore the application of K-modified graphene in electrochemistry, cyclic voltammetric characteristics of NO_2^- at the K-modified graphene electrode were investigated. As can be seen, the bare GCE exhibited an oxidation process to 5 mM NO_2^- at potentials more positive than +0.65 V in 0.1 M pH 7.4 phosphate buffered saline (PBS) at a scan rate of 50 mV s^{-1} (curve b, **Figure 8**), which corresponds to the conversion of NO_2^- to NO_3^- through a two-electron oxidation process:[41]

$NO_2^- + H_2O \rightarrow NO_3^- + 2H^+ + 2e^-$.

The oxidation current was rather weak due to the slow electron transfer kinetics of nitrite oxidation process. However, in comparison with that at the bare GCE, a remarkable increase in oxidation peak could be observed at around +0.75 V with the initial potential of +0.55 V at the K-modified graphene/GCE (curve d, Figure 8). And, the oxidation peak current was 218.7 μA. The parallel experiment with graphene was carried out to confirm the contribution of K modification to the high electrocatalytic activity of NO_2^- at the K-modified graphene electrode. For the graphene/GCE, only a small oxidation peak was observed at +0.79 V with the initial potential of +0.60 V (curve c, Figure 8). The results demonstrated that K modification in graphene play a key role in enhancing the electrocatalytic activity of the graphene to NO_2^-. Inset of Figure 8 shows the cyclic voltammograms of graphene and K-modified graphene in 0.1 M pH 7.4 PBS acquired at a scan rate of 50 mV s^{-1}. The higher capacitance current at the K-modified graphene GCE may result from its more fluctuant surface of K-modified graphene as Figure 4B showed.

2.3. Application of K-Modified Graphene in Nitrite-Selective Sensing

Figure 9 depicts the typical amperometric response of the K-modified graphene upon successive addition of different concentrations of NO_2^- in 0.1 M PBS (pH 7.4) at an applied potential of +0.75 V. The response reached a steady signal within only 2 s and displayed a linear increase with the increasing concentration from 0.5 μM to 7.8 mM, with a detection limit of 0.2 μM at a signal-to-noise ratio of 3. The linear response range was wider than 5 μM to 6.75 mM at the graphene/poly-cyclodextrin/MWNT-modified electrode[77] and 50 μM to 2.5 mM at the single-layer graphene nanoplatelet/protein-composite-modified electrode.[78] In addition, the detection limit was lower than 1.65 and 10 μM[77,78] at the respective modified electrodes, indicating that K-modified graphene is an excellent choice for the enhanced electrochemical sensing.

The sensor for NO_2^- showed good fabrication reproducibility with a relative standard deviation (RSD) of 3.17% estimated from the slopes of the calibration plots at five freshly prepared K-modified graphene modified GCEs. The batch-to-batch reproducibility

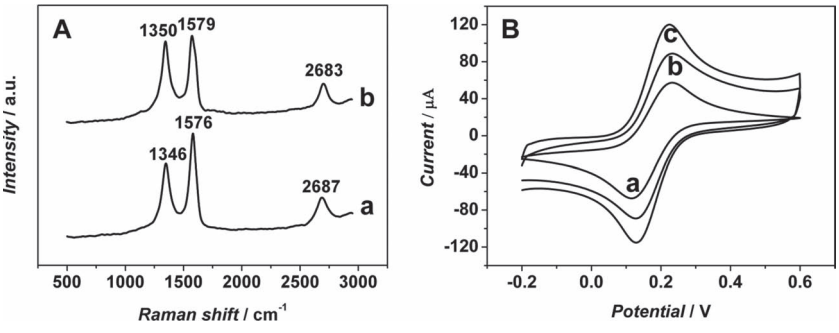

Figure 7. A) Raman spectra of graphene (a) and K-modified graphene (b). B) Cyclic voltammograms of bare/GCE (a), graphene/GCE (b), and K-modified graphene/GCE (c) in 0.1 M KCl solution containing 5 mM $K_3[Fe(CN)_6]/K_4[Fe(CN)_6]$. Scan rate: 50 mV s^{-1}.

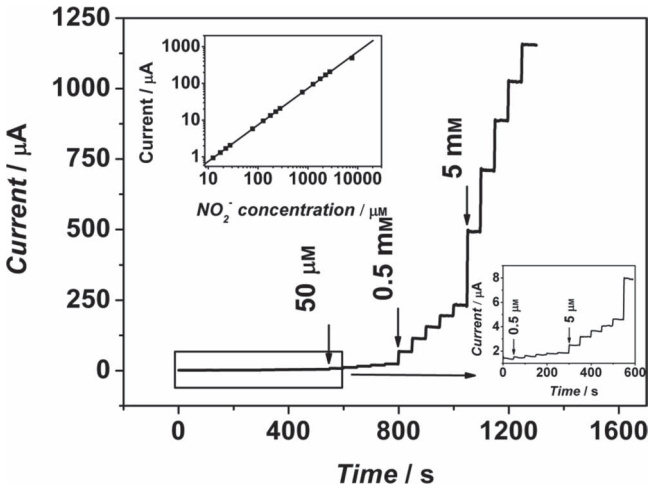

Figure 9. Successive amperometric response of K-modified graphene/GCE to NO_2^- in 0.1 M pH 7.4 PBS at an applied potential of +0.75 V. Upper inset: linear calibration curve; lower inset: amplified response.

showed a RSD of 3.43% for the slopes of the calibration plots obtained from five independently prepared sensors. Additionally, at NO_2^- concentrations of 5 and 500 μM, the sensor showed good repeatability with the RSDs of 3.21% and 2.95% examined for five determinations, respectively. When the sensor was not in use, it was stored in shade at room temperature and periodically measured (see Figure S1, Supporting Information). No obvious decrease in the amperometric response to 5 and 500 μM NO_2^- was observed after one week. It was able to retain 95.0% of its initial amperometric response after a month. This implies that the K-modified graphene can be used as a stable sensor.

The effects of common interfering species on the sensing response were examined (see Table S1, Supporting Information). Anions (F^-, Cl^-, Br^-, CO_3^{2-}, HCO_3^-, ClO_3^-, ClO_4^{2-}, PO_3^{3-}, HPO_3^{2-}, $H_2PO_3^-$, NO_3^-, SO_4^{2-}), cations (Na^+, K^+, Ca^{2+}, Mg^{2+}, Zn^{2+}, Cu^{2+}, Cd^{2+}, NH_4^+), and saccharides (glucose, sucrose, fructose) at 100 times the concentration of NO_2^- did not interfere with the amperometric response to NO_2^-. Ascorbic acid, uric acid, lactic acid, and glutamic acid could be tolerated at less than a twofold concentration of NO_2^-. Hydrogen peroxide (H_2O_2) could be tolerated at less than 20 times the concentration of NO_2^-. Good selectivity and sensitivity of K-modified graphene for NO_2^- sensing suggests its potential application as an advanced material in electrochemical sensors and biosensors.

2.4. Determination of NO_2^- Released From HL-60 and SMMC-7721 Cancer Cells

To evaluate the practical applicability, the sensor was used to determination of the concentrations of NO_2^- released from HL-60 and SMMC-7721 cancer cells. The results indicated that NO_2^- concentrations from HL-60 and SMMC-7721 cells (10^5 cells cm^{-2}) are ca. 0.70 and 0.90 μM in the absence of lipopolysaccharide (LPS) (**Figure 10**) in 0–6 days, and the values were almost consistent. Furthermore, the developed method was also used to measure NO_2^- released from LPS treated HL-60 and SMMC-7721 cells. Figure 10 shows the time course experimental results with LPS loading. These concentrations of NO_2^- released from HL-60 and SMMC-7721 cells are significantly increased after treatment with 50 ng mL^{-1} LPS for 1–4 days and reached the relatively stable values (ca. 8.0 and 9.0 μM) at 4–6 days. Therefore, the proposed method could be used to study the cellular kinetics of NO_2^-.

To evaluate the validity of the NO_2^- concentrations produced by HL-60 and SMMC-7721 cells detected with the developed method, recovery testing was carried out. Three samples with different concentrations of HL-60 and the other three samples with different concentrations of SMMC-7721 cells were prepared and specific amounts of NO_2^- (2, 5, and 10 μM) were added to these samples. The average recoveries were 101.1%, 100.9%, and 103.1% (from HL-60 cell) and 102.3%, 101.5%, and 102.8% (from SMMC-7721 cell), and the RSDs were 3.19%, 2.70%, and 3.67% and 3.43%, 3.03%, and 2.96%, respectively (five measurements). This indicates that the developed approach has high accuracy in measuring NO_2^- concentrations released from HL-60 and SMMC-7721 cells. These observations substantially demonstrate that the developed method represents a new sensing platform for reliable and durable determination of NO_2^- in vitro and from cancer cells and could be potentially useful for further physiological and pathological investigations.

3. Conclusions

In conclusion, we have presented the first report on a facile and mild methodology for synthesizing K-modified graphene using the room-temperature chemical method. The proposed method is unique in its simplicity and controllability. The as-prepared K-modified graphene, as an advanced electrode material, was successfully employed as an NO_2^- amperometric sensor, exhibiting a low detection limit and high sensitivity. In particular, the developed sensor could be further applied in the determination of NO_2^- in vitro and released from liver cancer and leukemia cells. We believe that the procedure described here to synthesize the K-modified graphene derived from the different types of K species (mainly K oxides, K ions, and K metal) into the graphene can be considered a general approach and can be

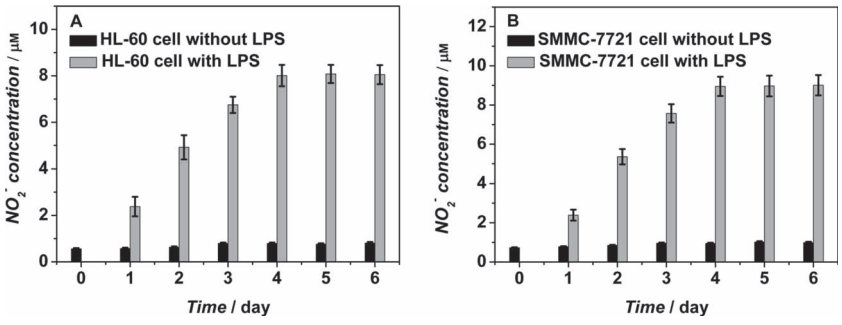

Figure 10. Time-dependent concentration of NO_2^- released from A) HL-60 and B) SMMC-7721cells (10^5 cells cm^{-2}) after treatment without (black bar) and with (light gray bar) 50 ng mL^{-1} LPS.

extended to the chemical modification of other alkali metals, enabling the formation of the most variations of graphene to fulfill the intrinsic modification of graphene and promoting applications in addressing various electrochemical issues, such as electrochemical sensing and biosensing, energy conversion, biomedical, and other electronic systems.

4. Experimental Section

Materials and Reagents: Graphite powder (99.9%, 325 mesh) was purchased from Alfa Aesar (China). Potassium (K), phenanthrene (98%), 1, 2-dimethoxyethane (99.5%, 1, 2-DME), β-D-glucose, L-ascorbic acid, uric acid, lactic acid, glutamic acid,and lipopolysaccharide (LPS) were obtained from Sigma–Aldrich (USA). Sodium nitrite (99.99%, $NaNO_2$), H_2SO_4, HCl, $K_2S_2O_8$, P_2O_5, $KMnO_4$, and hydration hydrazine (80%) were purchased from Nanjing Chemical Reagent Co. Ltd. (China). Hydrogen peroxide (H_2O_2) (30%) was purchased from Shanghai Chemical Reagent Co. Ltd. (China). All other chemical materials were of analytical grade and used without further purification in experiments. Ultrapure water, which was obtained from a Milli-Q water purifying system, was used for preparation of all aqueous solutions.

Instrumentation: TEM images were collected using a JEOL JEM-3011 transmission electron microscope. AFM images were collected using an atomic force microscope (Agilent 5500 model, USA) in tapping mode at room temperature. XPS measurements were performed with an Ultra Axis spectrophotometer (Kratos Analytical Ltd., Manchester, UK) equipped with a monochromatic Al Kα source operated at 150 W. Resonance Raman spectra were measured on a LabRAM HR 800 Raman spectrophotometer (Jobin Yvon, France). DC resistance measurements were carried out by the standard four-probe method using the resistivity option in a Physical Property Measurement System (PPMS) (Quantum Design, USA). Electrochemical measurements were performed on a computer-controlled electrochemical analyzer (CHI 660C, Shanghai Chenhua Apparatus, China) using a conventional three-electrode system with a glassy carbon electrode (GCE) as a working electrode, a platinum foil as an auxiliary electrode, and a saturated calomel electrode (SCE) as a reference electrode.

Synthesis of Graphene: Graphite powder (2 g) was put into a mixture of concentrated H_2SO_4 (12 mL), $K_2S_2O_8$ (3.0 g), and P_2O_5 (3.0 g). The solution was stirred at 80°C for 5 h. Next, the mixture was cooled to room temperature and diluted with deionized water (500 mL). The resulting product was filtered using 0.2 μm Nylon film and dried at room temperature. The preoxidized graphite was then reoxidized by the Hummers and Offeman method.[79] Pretreated graphite powder was put into 0 °C concentrated H_2SO_4 (150 mL), then $KMnO_4$ (25 g) was added gradually under stirring at around 5 °C. The mixture was stirred at 35 °C for 4 h and then diluted with ultrapure water (250 mL) keeping the temperature at 50 °C. Then, ultrapure water (1 L) was injected into the mixture followed by adding 30% H_2O_2 (30 mL). The mixture was filtered and washed with 1:10 HCl aqueous solution (1 L) to remove metal ions followed by 1 L of ultrapure water to remove the acid. The resulting product was dried in air atmosphere and diluted to make graphite oxide dispersion (0.5% w/w). Finally, it was purified by dialysis for one week to remove the remaining metal species. Exfoliation was carried out by sonicating 0.1 mg mL^{-1} graphite oxide dispersion under ambient conditions for 40 min. The resulting homogeneous yellow-brown dispersion was used for reduction. Reduction of graphene oxide was carried out by adding hydration hydrazine (80%, 5 mL) into 50 mL solution of 0.1 mg mL^{-1} graphene oxide and kept stirring for 24 h at 80 °C.[19,63] At last, black powder graphene was obtained by filtering the product and drying in vacuum.

Synthesis of Potassium-Modified Graphene and Preparation of its Modified Electrode: K-modified graphene was synthesized according to the chemical K-modifying at room temperature. The detailed preparation procedure is as follows. The phenanthrene/K solution complex was made by reacting K (10, 20, 40, 60, 80, 100 mg) with 0.2 M of phenanthrene (98%) in 20 mL of 1, 2-dimethoxyethane (1, 2-DME, 99.5%) solution. Then, the graphene (20 mg) were added to the phenanthrene/K solution complex for the K-modifying into graphene by π-stacking interaction between the graphene and phenanthrene. Finally, the reaction was conducted for 48 h with stirring using a magnetic bar at 500 rpm at room temperature. The resulting product was thoroughly washed several times with ethanol, and then dried at 60°C under air atmosphere.

The glassy carbon electrodes (GCE, d = 3 mm, ca. 0.07 cm^2) were polished to a mirror-like surface with 1.0 and 0.3 μm alumina slurry, ultrasonically washed in absolute ethanol and ultrapure water for 2 min, respectively, and dried at room temperature. A suspension of K-modified graphene (5 μL, 0.5 mg mL^{-1}) was applied to the GCE and dried at room temperature to obtain the K-modified graphene/GCE. Similarly, a graphene/GCE was prepared.

Determination of NO_2^- In Vitro: The concentrations of NO_2^- released from human leukemia (HL-60) and liver cancer (SMMC-7721) cells were determined using the K-modified graphene/GCE. Cells were cultured at 37 °C in Roswell Park Memorial Institute (RPMI) 1640 medium (GIBCO) supplemented with 10% (v/v) fetal bovine serum (FBS, GIBCO), 60 μg mL^{-1} penicillin, and 100 μg mL^{-1} streptomycin in a 5% CO_2 environment. After 24 h, the cells were collected and separated from the medium by centrifugation at 1000 rpm for 5 min and then washed twice with sterile PBS (pH 7.4). The sediment was resuspended in PBS to obtain a homogeneous cell suspension at a certain concentration. The cell number was determined using a Petroff Hausser cell counter (USA). For NO_2^- detection, cells were treated with 50 ng mL^{-1} of lipopolysaccharide (LPS) for a period of 0–6 days. Then, cells (10^5 cells cm^{-2}) were centrifuged and the cultured supernatants were collected and used for NO_2^- analysis. Each sample was analyzed in quintuplicate.

Supporting Information

Supporting Information is available from the Wiley Online Library or from the author.

Acknowledgements

The work was financial supported by the 973 Program (Grant Number 2012CB932600), the National Natural Science Foundation of China (Grant Number 21025522, 21135003, 20890020), and the National Natural Science Funds for Creative Research Groups (21121091) of China.

Received: December 14, 2011
Published online: February 17, 2012

[1] K. S. Novoselov, A. K. Geim, S. V. Morozov, D. Jiang, Y. Zhang, S. V. Dubonos, I. V. Grigorieva, A. A. Firsov, *Science* **2004**, *306*, 666.
[2] B. J. Choi, H. Park, T. J. Park, M. H. Yang, J. S. Kim, S.Y. Jang, N. S. Heo, S. Y. Lee, J. Kong, W. H. Hong, *ACS Nano* **2010**, *4*, 2910.
[3] X. Li, X. Wang, L. Zhang, S. Lee, H. Dai, *Science* **2008**, *319*, 1229.
[4] J. Lu, L. T. Drzal, R. M. Worden, I. Lee, *Chem. Mater.* **2007**, *19*, 6240.
[5] X. Wang, L. Zhi, K. Müllen, *Nano Lett.* **2008**, *8*, 323.
[6] F. Schedin, A. K. Geim, S. V. Morozov, E. W. Hill, P. Blake, M. I. Katsnelson, K. S. Novoselov, *Nat. Mater.* **2007**, *6*, 652.
[7] J. S. Bunch, A. M. Zande, S. S. Verbridge, I. W. Frank, D. M. Tanenbaum, J. M. Parpia, H. G. Craighead, P. L. McEuen, *Science* **2007**, *315*, 490.
[8] T. Ramanathan, A. A. Abdala, S. Stankovich, D. A. Dikin, M. Herrera-Alonso, R. D. Piner, D. H. Adamson, H. C. Schniepp, X. Chen, R. S. Ruoff, S. T. Nguyen, I. A. Aksay, R. K. Prud'Homme, L. C. Brinson, *Nat. Nanotechnol.* **2008**, *3*, 327.

[9] E. Yoo, J. Kim, E. Hosono, H. S. Zhou, T. Kudo, I. Honma, *Nano Lett.* **2008**, *8*, 2277.
[10] M. D. Stoller, S. Park, Y. Zhu, J. An, R. S. Ruoff, *Nano Lett.* **2008**, *8*, 3498.
[11] W. Chen, S. Chen, D. C. Qi, X. Y. Gao, A. T. S. Wee, *J. Am. Chem. Soc.* **2007**, *129*, 10418.
[12] S. P. Pang, H. N. Tsao, X. L. Feng, K. Müllen, *Adv. Mater.* **2009**, *21*, 3488.
[13] Z. S. Wu, S. F. Pei, W. C. Ren, D. M. Tang, L. B. Gao, B. L. Liu, F. Li, C. Liu, H. M. Cheng, *Adv. Mater.* **2009**, *21*, 1756.
[14] Y. F. Xu, Z. B. Liu, X. L. Zhang, Y. Wang, J. G. Tian, Y. Huang, Y. F. Ma, X. Y. Zhang, Y. S. A. Chen, *Adv. Mater.* **2009**, *21*, 1275.
[15] S. Watcharotone, D. A. Dikin, S. Stankovich, R. Piner, I. Jung, G. H. B. Dommett, G. Evmenenko, S. E. Wu, S. F. Chen, C. P. Liu, S. T. Neugen, R. S. Ruoff, *Nano Lett.* **2007**, *7*, 1888.
[16] E. Jin, X. F. Lu, L. L. Cui, D. M. Chao, C. Wang, *Electrochim. Acta* **2010**, *55*, 7230.
[17] X. L. Li, G. Y. Zhang, X. D. Bai, X. M. Sun, X. R. Wang, E. Wang, H. J. Dai, *Nat. Nanotechnol.* **2008**, *3*, 538.
[18] Y. Y. Shao, Y. Wang, H. Wu, J. Liu, I. A. Aksay, Y. H. Lin, *Electroanalysis* **2010**, *22*, 1027.
[19] Y. Wang, Y. Y. Shao, D. W. Matson, J. H. Li, Y. H. Lin, *ACS Nano* **2010**, *4*, 1790.
[20] Y. F. Li, Z. Zhou, P. W. Shen, Z. F. Chen, *ACS Nano* **2009**, *3*, 1952.
[21] H. Huang, S. Chen, X. Y. Gao, W. Chen, A. T. S. Wee, *ACS Nano* **2009**, *3*, 3431.
[22] D. W. Boukhvalov, M. I. Katsnelson, *Nano Lett.* **2008**, *8*, 4373.
[23] R. S. Sundaram, C. Gomez-Navarro, K. Balasubramanian, M. Burghard, K. Kern, *Adv. Mater.* **2008**, *20*, 3050.
[24] J. L. Vickery, A. J. Patil, S. Mann, *Adv. Mater.* **2009**, *21*, 2180.
[25] S. J. Guo, S. J. Dong, E. K. Wang, *ACS Nano* **2010**, *4*, 547.
[26] S. J. Guo, D. Wen, Y. M. Zhai, S. J. Dong, E. K. Wang, *ACS Nano* **2010**, *4*, 3959.
[27] S. Mao, G. Lu, K. Yu, Z. Bo, J. Chen, *Adv. Mater.* **2010**, *22*, 3521.
[28] W. Ren, Y. X. Fang, E. K. Wang, *ACS Nano* **2011**, *5*, 6425.
[29] J. L. Sabourin, D. M. Dabbs, R. A. Yetter, F. L. Dryer, I. A. Aksay, *ACS Nano* **2009**, *3*, 3945.
[30] T. O. Wehling, K. S. Novoselov, S. V. Morozov, E. E. Vdovin, M. I. Katsnelson, A. K. Geim, A. I. Lichtenstein, *Nano Lett.* **2008**, *8*, 173.
[31] L. S. Panchakarla, K. S. Subrahmanyam, S. K. Saha, A. Govindaraj, H. R. Krishnamurthy, U. V. Waghmare, C. N. R. Rao, *Adv. Mater.* **2009**, *21*, 4726.
[32] L. Liu, S. M. Ryu, M. R. Tomasik, E. Stolyarova, N. Jung, M. S. Hybertsen, M. L. Steigerwald, L. E. Brus, G. W. Flynn, *Nano Lett.* **2008**, *8*, 1965.
[33] Y. Y. Shao, S. Zhang, M. H. Engelhard, G. S. Li, G. C. Shao, Y. Wang, J. Liu, I. A. Aksay, Y. H. Lin, *J. Chem. Mater.* **2010**, *20*, 7491.
[34] G. Giovannetti, P. A. Khomyakov, G. Brocks, V. M. Karpan, J. van denBrink, P. J. Kelly, *Phys. Rev. Lett.* **2008**, *101*, 026803.
[35] M. Bianchi, E. D. L. Rienks, S. Lizzit, A. Baraldi, R. Balog, L. Hornekaer, P. Hofmann, *Phys. Rev. B* **2010**, *81*, 041403.
[36] N. Jung, B. Kim, A. C. Crowther, N. Kim, C. Nuckolls, L. Brus, *ACS Nano* **2011**, *5*, 5708.
[37] K. Y. Chun, C. J. Lee, *J. Phys. Chem. C* **2008**, *112*, 4492.
[38] X. L. Li, J. J. Xu, H. Y. Chen, *Electrochim. Acta* **2011**, *56*, 9378.
[39] M. Nielsen, L. H. Larsen, M. S. M. Jetten, N. P. Revsbech, *Appl. Environ. Microbiol.* **2004**, *70*, 6551.
[40] S. M. Silva, L. H. Mazo, *Electroanalysis* **1998**, *10*, 1200.
[41] S. Rajesh, A. K. Kanugula, K. Bhargava, G. Ilavazhagan, S. Kotamraju, C. Karunakaran, *Biosens. Bioelectron.* **2010**, *26*, 689.
[42] S. S. Mirvish, *Cancer Lett.* **1995**, *93*, 17.
[43] P. Wang, Z. B. Mai, Z. Dai, Y. X. Li, X. Y. Zou, *Biosens. Bioelectron.* **2009**, *24*, 3242.
[44] M. G. Almeida, C. M. Silveira, J. J. G. Moura, *Biosens. Bioelectron.* **2007**, *22*, 2485.
[45] R. Geng, G. H. Zhao, M. C. Liu, M. F. Li, *Biosens. Bioelectron.* **2008**, *29*, 2794.
[46] M. Grau, U. B. Hendgen-Cotta, P. Brouzos, C. Drexhage, T. Rassaf, T. Lauer, A. Dejam, M. Kelm, P. Kleinbongard, *J. Chromatogr. B* **2007**, *851*, 106.
[47] M. Zhang, D. X. Yuan, G. H. Chen, Q. L. Li, Z. Zhang, Y. Liang, *Microchim. Acta* **2008**, *160*, 461.
[48] S. M. Helmke, M. D. Duncan, *J. Chromatogr. B* **2007**, *851*, 83.
[49] C. Abha, K. B. Anil, V. K. Gupta, *Talanta* **2001**, *55*, 789.
[50] V. D. Matteo, E. Esposito, *J. Chromatogr. A* **1997**, *789*, 213.
[51] K. J. Huang, W. Z. Xie, H. S. Zhang, H. Wang, *Microchim. Acta* **2008**, *161*, 201.
[52] P. H. MacArthur, S. Shiva, M. T. Gladwin, *J. Chromatogr. B* **2007**, *851*, 93.
[53] R. Burakham, M. Oshima, K. Grudpan, S. Motomizu, *Talanta* **2004**, *64*, 1259.
[54] N. Bord, G. Cretier, J. L. Rocca, C. Bailly, J. P. Souchez, *J. Chromatogr. A* **2005**, *1100*, 223.
[55] W. W. Yang, Y. Bai, Y. C. Li, C. Q. Sun, *Anal. Bioanal. Chem.* **2005**, *382*, 44.
[56] D. Quan, R. K. Nagarale, W. Shin, *Electroanalysis* **2010**, *22*, 2389.
[57] W. L. Zhu, Y. Zhou, J. R. Zhang, *Talanta* **2009**, *80*, 224.
[58] J. F. Moulder, W. F. Stickle, P. E. Sobol, K. D. Bomben, *Handbook of X-ray Photoelectron Spectroscopy*, Perkin Elmer, Eden Prairie, MN **1992**.
[59] S. Li, E. T. Kang, K. G. Neoh, Z. H. Ma, K. L. Tan, W. Huang, *Appl. Surf. Sci.* **2001**, *181*, 201.
[60] R. Clement, in *Hybrid Organic-Inorganic Composites*(Eds: J. E. Mark, C. Y. C. Lee, P. A. Bianconi), American Chemical Society, Washington, DC**1995**.
[61] M. P. Seah, I. S. Gilmore, S. J. Spencer, *Surf. Interface Anal.* **2001**, *31*, 778.
[62] P. Y. Brisson, H. Darmstadt, M. Fafard, A. Adnot, G. Servant, G. Soucy, *Carbon* **2006**, *44*, 1438.
[63] D. Li, M. B. Müller, S. Gilje, R. B. Kaner, G. G. Wallace, *Nat. Nanotechnol.* **2008**, *3*, 101.
[64] W. W. Tu, J. P. Lei, S. Y. Zhang, H. X. Ju, *Chem. Eur. J.* **2010**, *16*, 10771.
[65] L. H. Tang, Y. Wang, Y. M. Li, H. B. Feng, J. Lu, J. H. Li, *Adv. Funct. Mater.* **2009**, *19*, 2782.
[66] C. S. Shan, H. F. Yang, J. F. Song, D. X. Han, A. Ivaska, L. Niu, *Anal. Chem.* **2009**, *81*, 2378.
[67] J. C. Meyer, A. K. Geim, M. I. Katsnelson, K. S. Novoselov, T. J. Booth, S. Roth, *Nature* **2007**, *446*, 60.
[68] Z. Jin, J. Yao, C. Kittrell, J. M. Tour, *ACS Nano* **2011**, *5*, 4112.
[69] C. Bower, S. Suzuki, K. Tanigaki, O. Zhou, *Appl. Phys. A* **1998**, *67*, 47.
[70] M. Zhou, Y. M. Zhai, S. J. Dong, *Anal. Chem.* **2009**, *81*, 5603.
[71] D. C. Wei, Y. Q. Liu, H. L. Zhang, L. P. Huang, B. Wu, J. Y. Chen, G. Yu, *J. Am. Chem. Soc.* **2009**, *131*, 11147.
[72] D. Graf, F. Molitor, K. Ensslin, C. Stampfer, A. Jungen, C. Hierold, L. Wirtz, *Nano Lett.* **2007**, *7*, 238.
[73] G. Eda, G. Fanchini, M. Chhowalla, *Nat. Nanotechnol.* **2008**, *3*, 270.
[74] S. Gilje, S. Han, M. Wang, K. L. Wang, R. B. Kaner, *Nano Lett.* **2007**, *7*, 3394.
[75] Y. J. Zhang, J. Li, Y. F. Shen, M. J. Wang, J. H. Li, *J. Phys. Chem. B* **2004**, *108*, 15343.
[76] X. Zhong, H. J. Bai, J. J. Xu, H. Y. Chen, Y. H. Zhu, *Adv. Funct. Mater.* **2010**, *20*, 992.
[77] Y. Zhang, R. Yuan, Y. Q. Chai, W. J. Li, X. Zhong, H. A. Zhong, *Biosens. Bioelectron.* **2011**, *26*, 3977.
[78] R. Yue, Q. Lu, Y. K. Zhou, *Biosens. Bioelectron.* **2011**, *26*, 4436.
[79] N. I. Kovtyukhova, P. J. Ollivier, B. R. Martin, T. E. Mallouk, S. A. Chizhik, E. V. Buzaneva, A. D. Gorchinskiy, *Chem. Mater.* **1999**, *11*, 771.